Energy for Sustainable Development 40 (2017) 41–49

Contents lists available at ScienceDirect

Energy for Sustainable Development

Study on methods to determine rotor equivalent wind speed to increase prediction accuracy of wind turbine performance under wake condition

Sanghyeon Jeon [a], Bumsuk Kim [b,*], Jongchul Huh [c]

[a] Hanjin IND. CO., LTD., Yangsan-daero, Habuk-myeon, Yangsan-si, Gyeongsangnam-do 1981-48, Republic of Korea
[b] Faculty of Wind Energy Engineering, Graduate school, Jeju National University, Jejudaehak-ro 102, Jeju-si, Jeju Special Self-Governing Province 690-756, Republic of Korea
[c] Department of Mechanical Engineering, Jeju National University, Jejudaehak-ro 102, Jeju-si, Jeju Special Self-Governing Province, 690-756, Republic of Korea

ARTICLE INFO

Article history:
Received 30 September 2016
Revised 9 February 2017
Accepted 24 June 2017
Available online xxxx

Keywords:
Wind turbine wake
Wake loss
Wind shear
Point wind speed
Rotor equivalent wind speed (REWS)

ABSTRACT

A downstream wind turbine located within the reach of the wake region of an upstream wind turbine experiences a decrease in power output due to wake effects. For this reason, when designing a wind farm, various engineering wake models are used to predict the power deficit and wind farm layout is designed in the optimal way to minimize the wake losses. Generally, in the process of calculating the loss of wind farm AEP, in most cases the single point-measured wind speed is used. However, this results in an error when predicting the loss of AEP under wake conditions. When predicting the AEP of a wind turbines affected by wakes, the rotor equivalent wind speed (REWS), which considers the effect of wake wind shear, should be applied. This research examined $REWS_{power}$ converted from the power output of a wind turbine to demonstrate the need of rotor equivalent wind speed under upstream turbine's wake condition and furthermore suggested a method to calculate $REWS_{spws}$ using the nacelle-measured wind speed. By analyzing 48 months collected data of Supervisory Control and Data Acquisition (SCADA) system from a wind farm, error percentages among $REWS_{power}$, $REWS_{spws}$, and the nacelle-measured wind speed were compared.

Introduction

As the capacity of wind turbines and the scale of wind farms grow, wake effects caused by neighboring turbines are becoming increasingly important. While the power deficit arising from these wake effects varies depending on the surrounding geographic environment and the wind farm layout, it is reported to be between 5 and 15% (Schepers et al., 2012). On an offshore wind farm in particular, the wind speed, which drops in the wind turbine behind, does not recover as fast as on an onshore wind farm, resulting in a higher loss in power output. When designing an offshore wind farm, it is therefore important to predict the loss of power output caused by wake effects and to optimize the layout design in order to minimize the loss. To determine wind turbine wake effects, a large number of engineering wake models have been developed, and many empirical studies have been conducted to increase and verify the prediction accuracy of such models.

David Ryan Van Luvanee and Thomas Sørensen et al. examined the Horns Rev. wind farm in Demark and conducted verification (VanLuvanee, 2006; Sørensen et al., 2008) of the prediction accuracy of engineering wake models, such as Jensen (1983), Katic et al. (1986), Ainslie Eddy Viscosity (1988), and Larsen (1988), which were implemented in the wind farm design software WindPRO (EMD International A/S). The results showed that the prediction accuracy of these wake models differed depending on changes in atmospheric stability and surface roughness. The simple N.O. Jensen wake model, which expresses wake changes in the form of a uniform velocity profile, was found to be most precise in its prediction results on sector averaged power.

R. J. Barthelmie et al. analyzed Supervisory Control and Data Acquisition (SCADA) data measured on the Danish offshore wind farms Nysted and Horns Rev. and compared (Barthelmie et al., 2010) the acquired wake loss values with values simulated by using engineering and research wake models developed by DTU-Riso, Garrad Hassan, ECN, and NTUA. The results showed that all of the wake models had a higher prediction accuracy of wake loss under high wind speed and full wake conditions than under low wind speed and partial wake conditions.

The EERA-DTOC Project (Gaumond et al., 2012) compared wake loss values measured from Horns Rev. and Lillgrund with those predicted by the N.O. Jensen, G. C. Larsen, and Fuga wake models, and found that the wake models overestimated wake loss. This may be because the wind speed decrease in the wake center is underestimated due to the high uncertainty of wind direction data. A study on how this uncertainty of

* Corresponding author.
E-mail address: bkim@jejunu.ac.kr (B. Kim).

http://dx.doi.org/10.1016/j.esd.2017.06.001
0973-0826/

measured wind direction data affects wake loss estimation is now being conducted by the IEA-Task 31: WakeBench Project (Moriarty et al., 2014).

Within the wake region of a wind turbine, a velocity deficit always occurs. The wind speed decreases most in the wake center region, and as the distance from the wake center increases, the speed gradually recovers until it reaches the ambient wind speed (Mckay et al., 2012). If the wake flow developed in the rear of an upstream wind turbine behind moves into a downstream wind turbine, the rotor disk of the downstream turbine is influenced by wake wind shear in the radial direction (horizontal and vertical direction). If only the single point wind speed measured at the height of a hub is applied when conducting power performance assessment on a downstream wind turbine influenced by wakes, it is highly likely that erroneous results will be obtained. For this reason, the representative wind speed, which incorporates wake wind shear, should be applied. As mentioned above, however, many previous studies have until now used the single point wind speed value to predict the power performance of a wind turbine located in the wake condition, so that the wake wind shear effect is not fully taken into account.

In this regard, many similar studies are being conducted on the application of the rotor equivalent wind speed (REWS) to increase measurement precision of the power performance of a wind turbine not influenced by wakes in which vertical wind shear only is being considered.

Rozenn Wagner and Clifton A. et al. measured the wind speed at five different heights in front of the rotor disk and presented a REWS calculation method (Wagner et al., 2009; Wagner et al., 2011; Clifton et al., 2013) using the average value calculated after segment weighting was applied to each height measured wind speed. The results of a comparison between the power curve where the REWS was applied and the actual power curve was far more accurate than using the point-measured wind speed. It was further verified by experimental method that the percentage error of prediction of the Annual Energy Production (AEP) could be reduced from −2.3% to −0.5%.

In addition, V. Barth et al. predicted the total AEP of a wind farm by using the REWS suggested by Rozenn Wagner and confirmed (Barth and Wassie Tsegai, 2014) that it provided results that were more accurate than those predicted by the point-measured wind speed. A method to measure the power performance using the REWS will be incorporated in a revision to IEC 61400–12-1 (2013).

As mentioned above, a working group is revising the international standard (IEC61400-12-1) with regard to the power performance test of a wind turbine. Therefore the standard only concerns wind turbines that are not influenced by wakes so that it only takes vertical wind shear into consideration.

However, when predicting the power performance of a wind turbine in the wind farm affected by wakes, the impact of wake wind shear, which is defined as the velocity gap between the wake center and wake flow edge, needs to be considered. In particular, to calculate wind farm power performance when verifying the prediction accuracy of various wake models, REWS that takes into account the effect of wake wind shear, rather than the single point decision wind speed calculated from wake models, needs to be introduced. As mentioned above, however, most previous studies have predicted the power performance of a wind turbine influenced by wakes by means of a wind speed acquired at a certain point from wake analysis results, and have verified wake models through comparison with measured data.

The results of verification of wake models could result in an error due to gaps in applied wind speed, so a thorough review is required on the differences in the single point wind speed and the REWS in the wake region of a wind turbine. Therefore, this study presents experimental results on gaps between $REWS_{power}$, calculated using the power curve measured from wind turbines in operation on a wind farm, and the point wind speed measured from the nacelle anemometer. Considering the REWS calculation method suggested by Rozenn Wagner, the study also provides a method to calculate $REWS_{spws}$, which uses the wind speed measured from the nacelle anemometer, and verifies its applicability through comparison with $REWS_{power}$.

Wind farm layout information and SCADA data classification

Wind farm measured for the study

The nacelle wind speed and power curve used in this study were acquired through analysis of SCADA data measured from operational wind turbines on the Sungsan wind farm. The Sungsan wind farm, operated by Korea Southern Power Co., Ltd. (KOSPO), is a 20 MW onshore wind farm located on Jeju Island and has 10 VESTAS V80–2 MW turbines with a hub height and rotor diameter of 80 m. Unlike most wind farms designed on a rectangular layout, this site has wind turbines installed at irregular intervals, so the layout is favorable for wake impact assessment according to changes in separation distance.

S.H. Jeon et al. (2015) used SCADA data obtained from the Sungsan wind farm (over 38 months) and conducted research (Jeon et al., 2015) on the verification of prediction accuracy of engineering wake models under single wake conditions. They showed that differences in the prediction accuracy of the models depended on the speed of the wind blowing into upstream wind turbines as well as changes in downstream distance. This study categorized SCADA data with a method identical to that of previous studies and utilized data gathered over 48 months in order to reduce uncertainty in the measured data.

Fig. 1 illustrates the wind turbine layout of the Sungsan wind farm. Seven wind turbines (WT03–WT09) are paired in four separation distances, and these distances were defined as the downstream distances (x). As shown by the dotted lines in the figure, the straight line connecting the hub center points of two wind turbines, when upstream and downstream turbines are located on a straight line with wind direction, is defined as the wake center line (x_{wcl}).

Table 1 shows separation distances of paired wind turbines. The wind turbines located upstream of the wake center line (WT04, WT06, WT07, WT09) were operated without being influenced by wakes while the wind turbines located downstream (WT03, WT05, WT07, WT08) were operated under the influence of wakes. Exceptionally, WT07 is defined as a wind turbine located upstream of WT08 under the condition of $x = 2.55D$ (rotor diameter), and located downstream of WT04 under the condition $x = 5.1D$.

SCADA data categorization depending on changes in relative offset angle

The SCADA data acquired on the Sungsan wind farm was analyzed in order to examine gaps in $REWS_{power}$ converted from power output, and the single point wind speed measured from the nacelle anemometer. The results of comparison depending on the distance between upstream and downstream wind turbines and changes in free stream wind speed are then presented.

The SCADA data was categorized into three key wind speed ranges measured from the nacelle anemometer at upstream wind turbines: 7 m/s (6.5 m/s–7.5 m/s), 9 m/s (8.5 m/s–9.5 m/s), and 11 m/s (10.5 m/s–11.5 m/s). Because power output of wind turbine corresponds to the kinetic energy flux through the swept rotor area, power output data from downstream wind turbines collected in the same time converted into $REWS_{power}$. For conversion of $REWS_{power}$ in downstream wind turbines, the individual power curves measured for 48 months excluding affected time of wake from neighboring wind turbine were used. The wind speed range under 7 m/s and above 11 m/s were excluded from data analysis as they were affected by blade pitch control needed for cut-in operation and power regulation, which made it incomparable in comparison between the nacelle wind speed and $REWS_{power}$.

The nacelle wind speed and $REWS_{power}$ of downstream wind turbines being affected by wakes were compared and examined for four

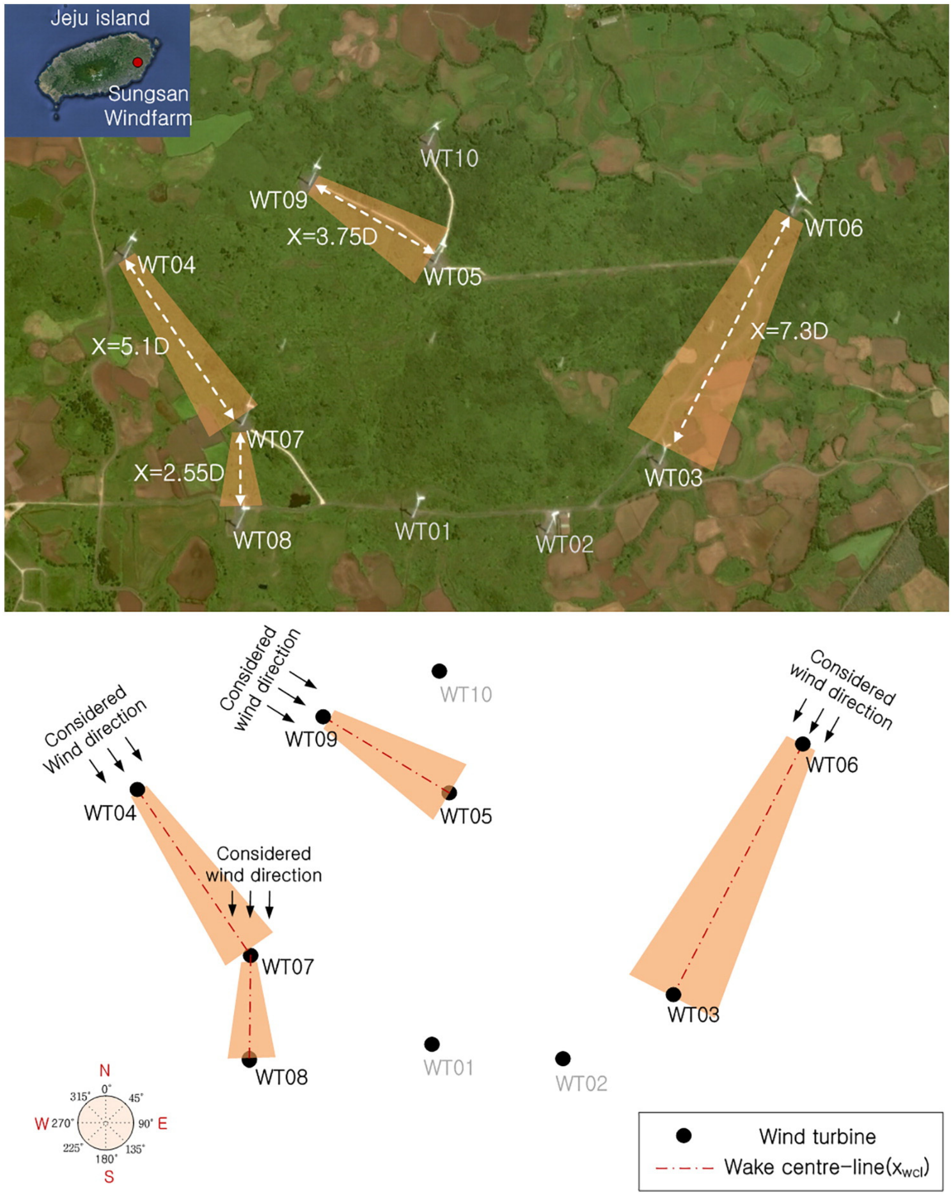

Fig. 1. Layout of the Sungsan wind farm and wind turbine pairs based on the separation distance. (Jeon et al., 2015)

separation distances. Table 1 shows separation distance information on combinations of paired upstream and downstream wind turbines.

Fig. 2 conceptually illustrates the relationship of the relative offset angle (θ_{rel}) between upstream and downstream wind turbines, which changes in accordance with an incoming wind direction.

As indicated in Fig. 2 (a), θ_{rel} is defined as 0° under the condition in which the wind direction and the wake center line are the same. In such a case, a downstream wind turbine is situated on the wake center of an upstream turbine. However, when θ_{rel} changes as the wind direction alters, as shown in Fig. 2 (b)–(d), a downstream turbine is located at a certain distance (r) from the wake center of an upstream turbine. Therefore, the separation (R) and downstream (x) distances between two wind turbines are identical under the condition where θ_{rel} is 0°, but as the wind direction changes, the downstream distance between the two wind turbines gradually diminishes. In order to measure the power performance of downstream wind turbines according to changes in wind direction, the change in θ_{rel} was set at 2° intervals from the wake center line. As the wind speed deficit was relatively large near the wake center area, the change in θ_{rel} was segmented and set at 1° intervals in order to more accurately capture changes in the power performance and $REWS_{power}$ of downstream wind turbines.

Table 1
Separation distance of wind turbine pairs (D: rotor diameter)(Jeon et al., 2015).

Separation distance	Wind turbine pairs
2.55*D*	WT07: Free stream condition WT08: Under WT07's wake condition
3.75*D*	WT09: Free stream condition: WT05: Under WT09's wake condition
5.1*D*	WT04: Free stream condition: WT07: Under WT04's wake condition
7.3*D*	WT06: Free stream condition: WT03: Under WT06's wake condition

Fig. 3 shows changes in downstream distance (x) and distance from the wake center (r) according to changes in θ_{rel} under the condition where the separation distance is 2.55*D*. As θ_{rel} increases, the downstream distance decreases while r increases. For example, the downstream distance decreased from 204 m ($\theta_{rel} = 0°$) to 176 m ($\theta_{rel} = 30°$) while r increased from 0 m to 102 m.

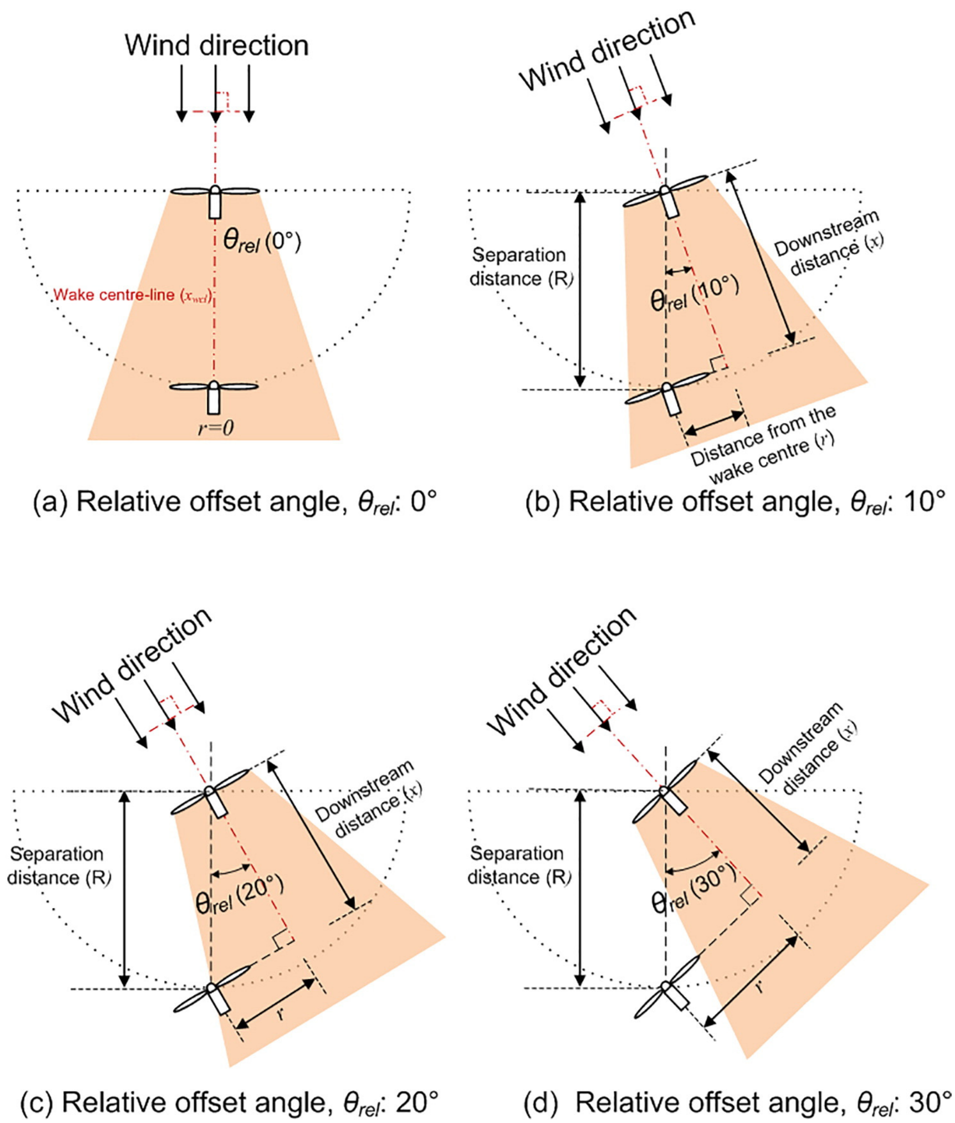

Fig. 2. Changes in the distance from wake center and the downstream distance in accordance with vary in the relative offset angle between upstream and downstream turbines.

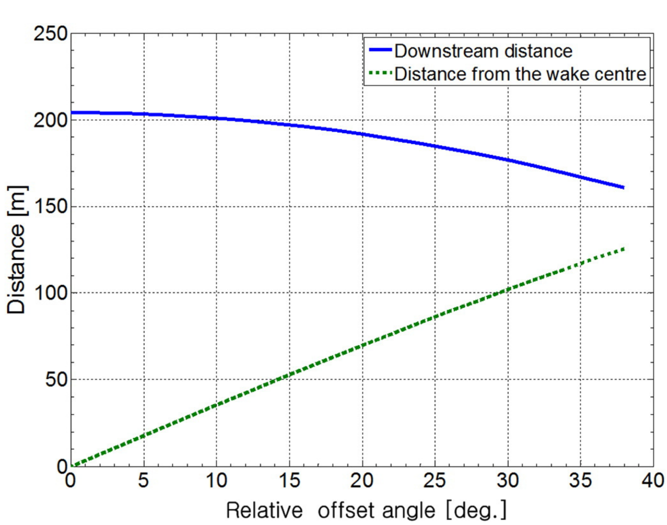

Fig. 3. Decreasing downstream distance and increasing distance from the wake center according to changes in relative offset angle.

Results and discussions

Comparison of the nacelle wind speed and $REWS_{power}$ of wind turbines affected by wake

The differences in nacelle wind speed and $REWS_{power}$ measured from downstream wind turbines affected by wake in accordance with changes in incoming wind speed and separation distance were analyzed.

Figs. 4–6 show the results of comparison between the nacelle wind speed and $REWS_{power}$ measured for each separation distance (2.55*D*–7.30*D*) under conditions in which the incoming wind speed was 7 m/s, 9 m/s, and 11 m/s.

Fig. 4 shows the results of comparison for an incoming wind speed towards an upstream wind turbine of 7 m/s, and the largest gap existed between the nacelle wind speed and $REWS_{power}$ in the wake center area. When |r| increases as the wind direction changes, the gap between the two wind speeds gradually narrows. Almost no gap exists between the two wind speeds under the condition where the downstream wind turbine is completely outside the wake region of the upstream wind turbine.

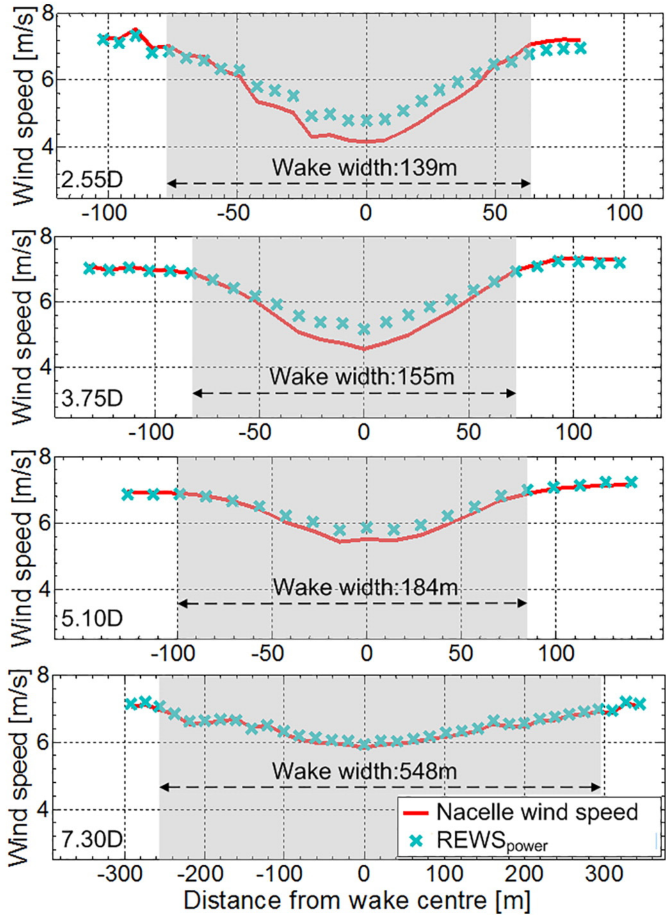

Fig. 4. Profile comparison between nacelle wind speed and $REWS_{power}$ ($V_{freestream}$: 6.5 m/s–7.5 m/s).

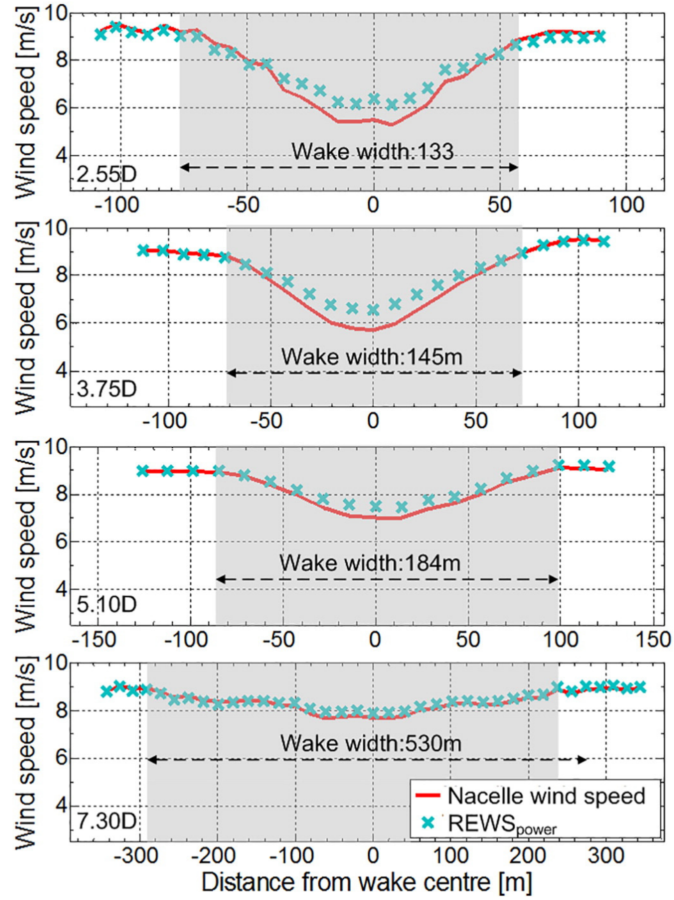

Fig. 5. Profile comparison between nacelle wind speed and $REWS_{power}$ ($V_{freestream}$: 8.5 m/s–9.5 m/s).

Under the condition in which separation distance = 2.55*D*, the wake width was 139 m, and it increased as the separation distance increased. Under the furthest separation distance of 7.30*D*, the wake width was 548 m. Moreover, the gap between the nacelle wind speed and $REWS_{power}$ decreased as the separation distance increased, and under the separation distance condition of 5*D* or greater, the wind speeds tended to become almost identical.

Fig. 5 shows the results of comparison of changes in wake wind speed profile under the incoming wind speed condition of 9 m/s. Similar to the results for 7 m/s, the largest gap between the two wind speeds exists in the wake center area, and as a downstream wind turbine become farther away from the wake effects of an upstream wind turbine, the gap narrows significantly.

Fig. 6 shows the results of comparison under the incoming wind speed condition of 11 m/s. While the tendency regarding the gap between the nacelle wind speed and $REWS_{power}$ was identical to that for the other conditions, the difference in quantitative value of the gap between the two wind speeds was smaller than that for the other conditions. This is because the rate of decline of wind speed in the wake center region is lower as the incoming wind speed increases (Machielse et al., 2007), and the wind shear become relatively small as the difference in wind speed between the wake center region and the surrounding areas decreases. Based on these findings, a conclusion can be drawn that almost no gap exists between the nacelle wind speed as the point-measured wind speed and $REWS_{power}$ as the average wind speed of a rotor disk, under conditions in which the incoming wind speed is high or the downstream distance is equal to or greater than 5D.

Fig. 7 shows changes in wake width in accordance with the separation distance at each wind speed. As can be seen from the figure, when the incoming wind speed is high, the wake width tends to become narrow (Machielse et al., 2007). As the separation distance increases, the wake width also increases, and it increases rapidly when the downstream distance is 5.1*D* or greater. This shows that the mixing effect between the wake and the surrounding flow is sufficiently activated. For this reason, it is difficult to clearly distinguish the boundaries of the wake region when the downstream distance is 7*D* or greater.

Generally, the recommended separation distance between wind turbines on an onshore wind farm is given as 6*D*–10*D* (Sanderse, 2009). This refers to a recommended separation distance in which the wind speed can recover as the wake flow developing in the rear of a wind turbine spreads downstream and is mixed with surrounding flow. The results of this study, in which the gaps between the two wind speeds for downstream distances of 5.1*D* or greater and wake profile changes were compared, confirm this recommendation.

Comparison of nacelle wind speed and $REWS_{power}$ of upstream and downstream turbines in the wake center region

Figs. 8–10 show the results of comparison between the nacelle wind speed and $REWS_{power}$ measured from upstream and downstream wind turbines. In order to analyze in more detail the wind speed gap in the wake center region where the gap between the nacelle wind speed and $REWS_{power}$ tended to be relatively large, the examined wake region was limited to 1*D* (80 m) and θ_{rel} was divided more narrowly into 1°

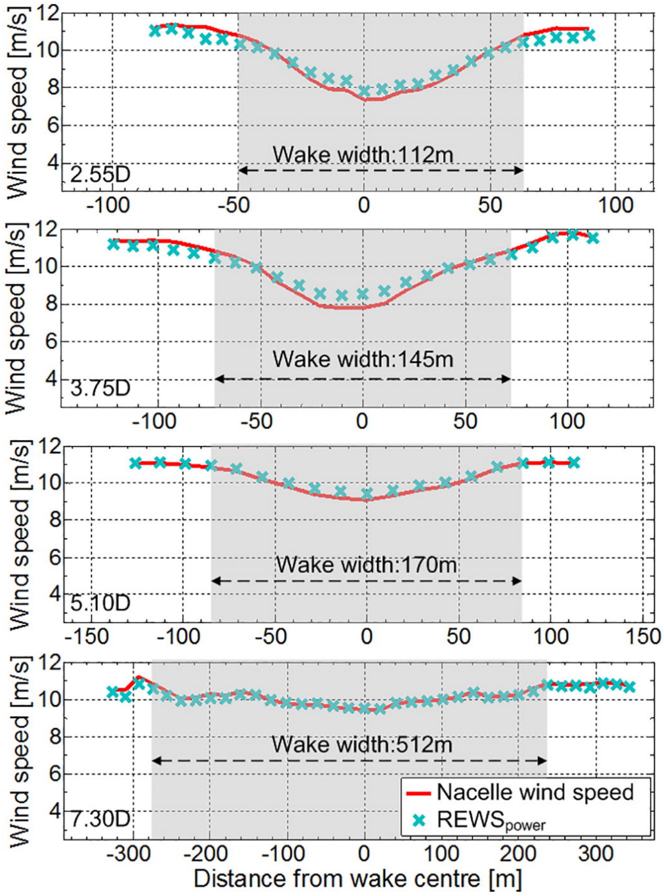

Fig. 6. Profile comparison between nacelle wind speed and $REWS_{power}$ ($V_{freestream}$: 10.5 m/s–11.5 m/s).

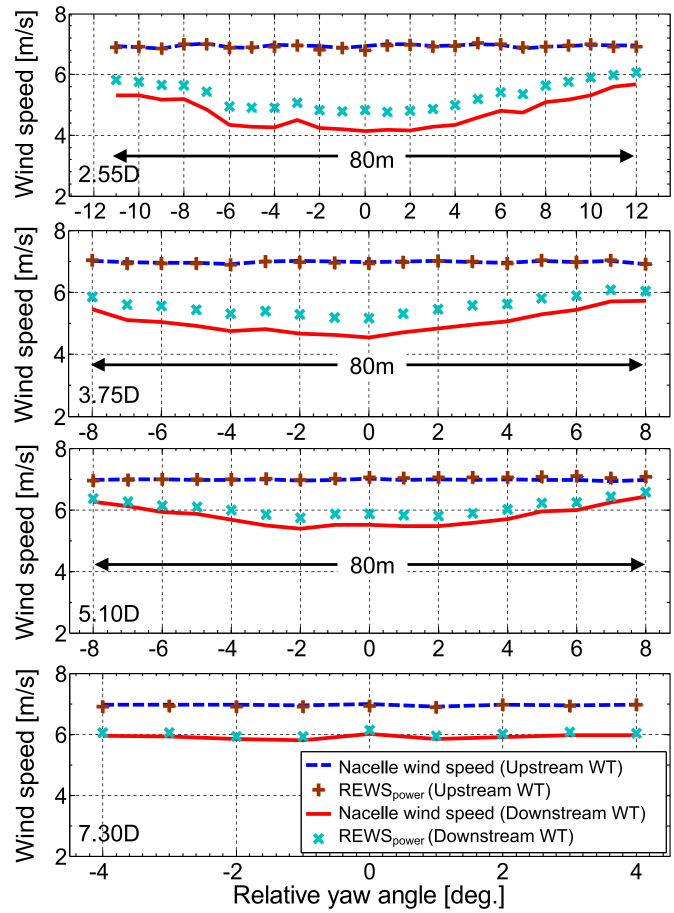

Fig. 8. Profile Comparison between $REWS_{power}$ and the nacelle wind speed of upstream and downstream wind turbines ($V_{freestream}$: 6.5 m/s–7.5 m/s).

intervals. As mentioned above, the gap between the nacelle wind speed and $REWS_{power}$ decreases as the separation distance increases and the incoming wind speed increases. For a separation distance of 7.3*D*, the two wind speeds were almost identical for all wind conditions. On the other hand, considering upstream wind turbines, it was found that regardless of changes in θ_{rel}, there was almost no gap between the nacelle wind speed and $REWS_{power}$ under all conditions. As upstream wind turbines are not affected by wakes, there exists no wake wind

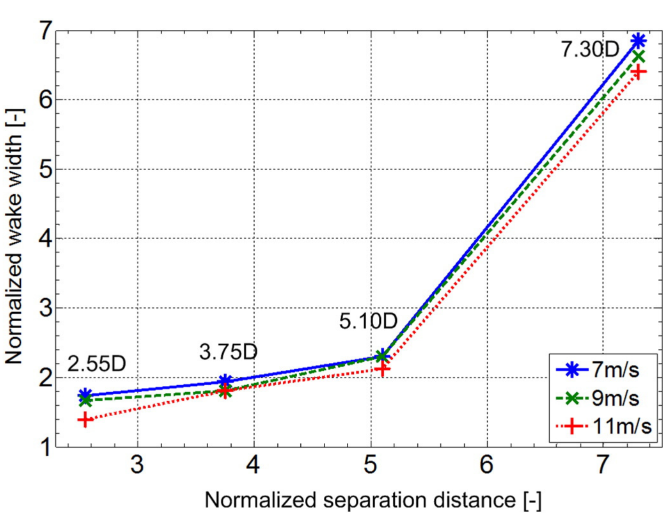

Fig. 7. Changes in wake width per wind speed according to an increase in separation distance.

shear in the upcoming wind speed. Therefore, it is feasible that no gap exists between the nacelle wind speed and $REWS_{power}$, and it can be confirmed that a gap between the two wind speeds in downstream turbines is largely affected by wake wind shear. Such wake wind shear effects appear relatively large until the downstream distance reaches 5.1*D*, but the gap is small for downstream distances greater than this.

In Fig. 11, the gap occurring between the two wind speeds as the separation distance increases is shown as a percentage. Under conditions in which the incoming wind speed was 7 m/s and 9 m/s and the separation distance was under 5.1*D*, the gap between the nacelle wind speed and $REWS_{power}$ was a maximum of over 9%, while it was less than 3% for a separation distance of 7.3*D*. As a large percentage error exists between the point-measured wind speed and the average rotor disk wind speed in the near wake region, it is recommended to apply $REWS_{power}$ when calculating the AEP of a wind turbine affected by wakes within 5.0*D*.

Proposed method to calculate a downstream wind turbine's $REWS_{spws}$ using the nacelle wind speed

As $REWS_{power}$ used in this study was converted and calculated from the measured power curve of wind turbines actually affected by wakes, it is difficult to apply without SCADA data recorded over a long time period. In order to enhance the accuracy of AEP calculation results from wind turbines influenced by wakes, in this section a method is proposed to calculate $REWS_{spws}$ that considers wake wind shear at a hub height by using the REWS calculation method discussed in a revision to IEC61400-12-1. In addition, the results of comparison of $REWS_{spws}$ and $REWS_{power}$ are presented to verify the applicability of the suggested method.

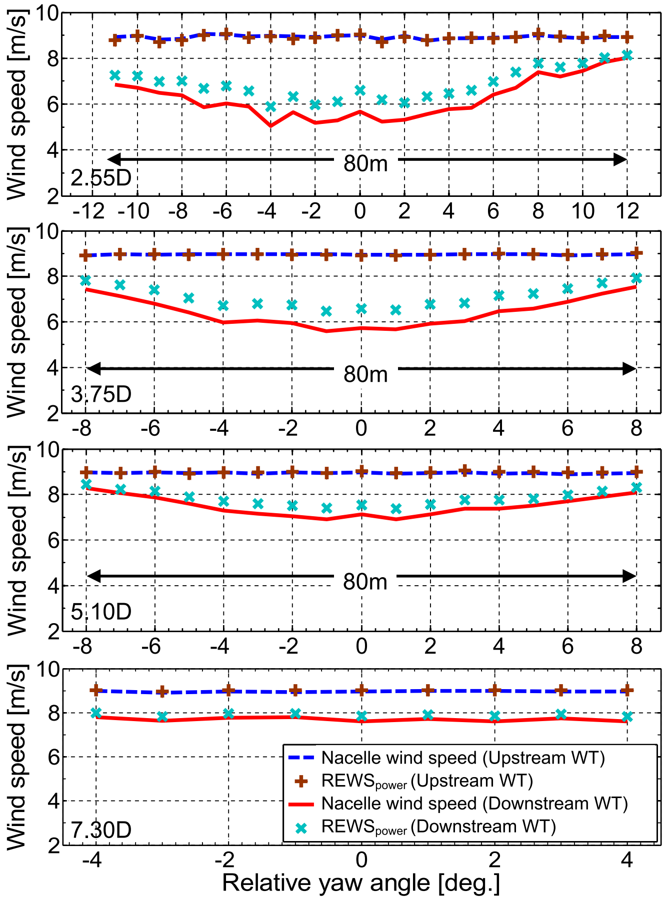

Fig. 9. Profile Comparison between $REWS_{power}$ and the nacelle wind speed of upstream and downstream wind turbines ($V_{freestream}$: 8.5 m/s–9.5 m/s).

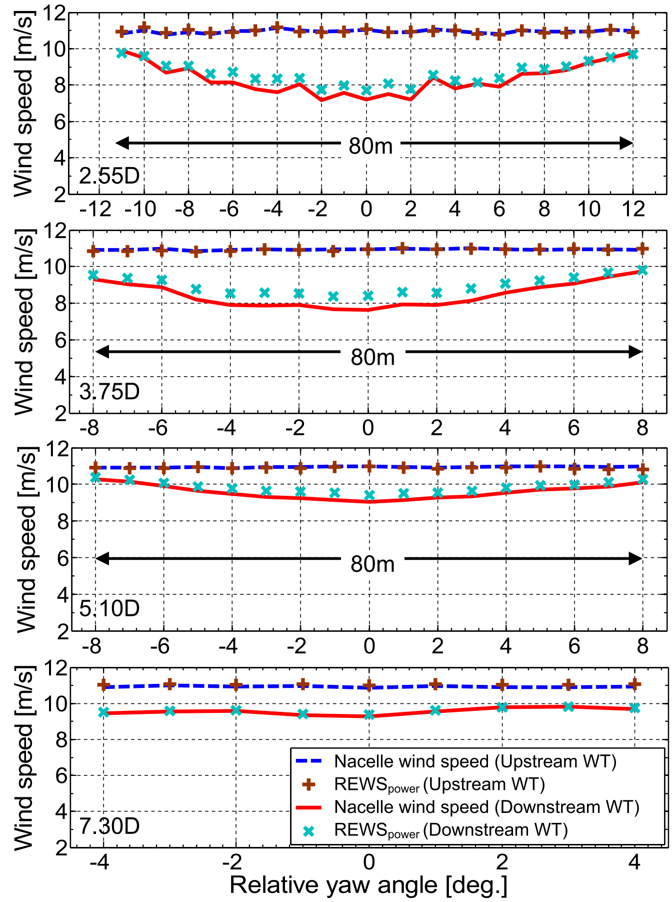

Fig. 10. Profile Comparison between $REWS_{power}$ and the nacelle wind speed of upstream and downstream wind turbines ($V_{freestream}$: 10.5 m/s–11.5 m/s).

The REWS calculation method discussed in IEC61400-12-1 is designed to measure the power performance of wind turbines not affected by wakes. It splits a rotor disk in the horizontal direction and considers wind shear in the vertical direction. The REWS is calculated by using the average derived after segment weighting is assigned to point-measured wind speeds in segmented areas.

However, as the method of splitting segments described by Rozenn Wagner or the IEC standard only incorporates wind shear depending on changes in height, and therefore it is not appropriate to reflect wake wind shear taking place in the wake region. Therefore, to consider the effect of wake wind shear that occurs on the rotor disk of a downstream wind turbine, in this study a method is proposed to split segments not horizontal but vertical direction as demonstrated in Fig. 12 (a). The rotor disk in this case is divided into four segments (S_1, S_2, S_3, and S_4) in total. The nacelle wind speeds of a downstream wind turbine measured at 10 m and 30 m along the horizontal axis from the hub center are applied as the wind speed representing each split segment. These representing wind speeds located in the horizontal direction at 10 m and 30 m are the nacelle wind speeds measured in accordance with changes in relative offset angle (θ_{rel}) as shown in Fig. 12 (b). Finally, the $REWS_{spws}$ suggested in this study can be calculated by Eq. (1) as illustrated below.

$$v_{eq} = \left(\sum_{i=1}^{n} v_i^3 \frac{A_i}{A} \right)^{1/3} \quad (1)$$

In this equation, n stands for the number of split segments or wind speed measurement points, v_i the representative wind speed measured from a split segment, A the swept area of a rotor disk, and A_i the area of a split segment.

Table 2 describes the split segments of a rotor disk and segment weighting used in this study. A segment weighting of 12.5% was applied to the wind speed at a point 10 m from the hub center and 37.5% was applied to the wind speed at a point 30 m away.

Figs. 13–15 show the results of comparison on $REWS_{spws}$, which is calculated by using the nacelle wind speed and $REWS_{power}$ converted from the wind turbine power in accordance with changes in the incoming wind speed and θ_{rel}.

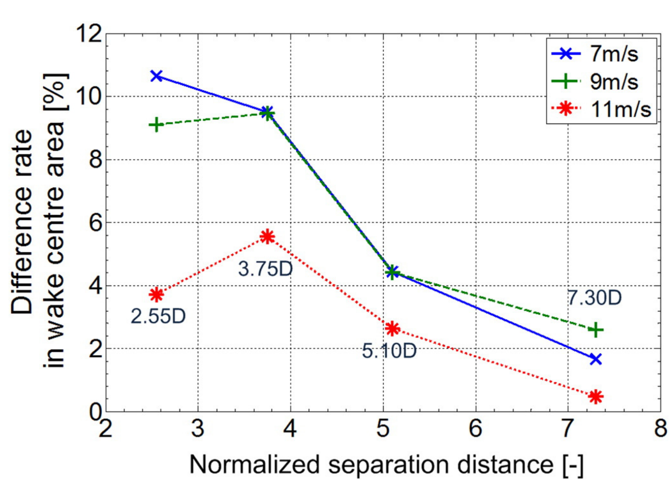

Fig. 11. Gap between nacelle wind speed and $REWS_{power}$ at the wake center ($\theta_{rel} = 0°$) according to an increase in separation distance.

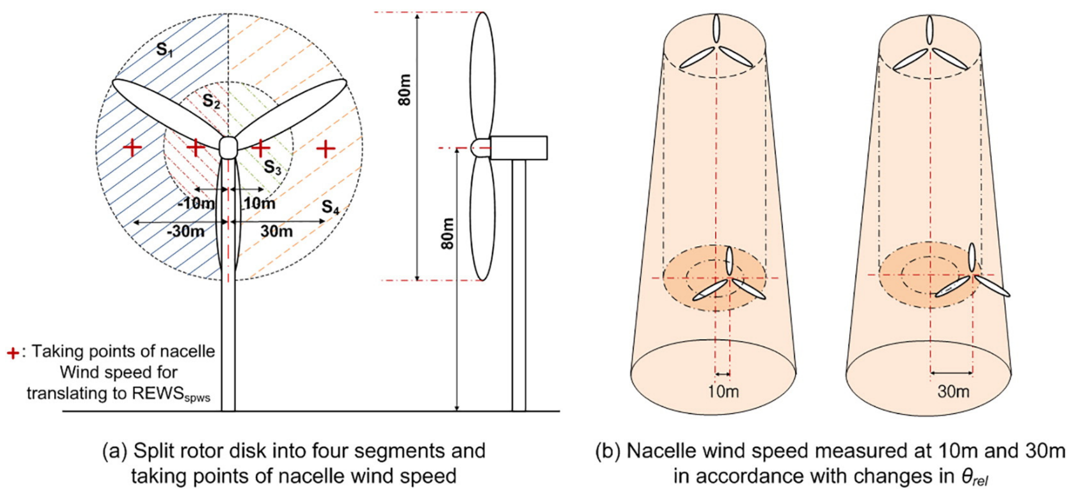

Fig. 12. Rotor area segments and acquisition points of representative wind speed.

While $REWS_{spws}$ and $REWS_{power}$ showed corresponding values when the incoming wind speeds were 7 m/s and 9 m/s, $REWS_{spws}$ showed lower values under all separation distance conditions when the speed was 11 m/s. This is because the same segment weighting as that for the other wind speed conditions was applied under high wind speed conditions, even though there were no significant changes in wake wind shear. It is therefore believed that the rotor disk should be divided into smaller segments in order to increase the prediction accuracy of $REWS_{spws}$ under high wind speed conditions. As demonstrated above, while the method to calculate $REWS_{spws}$ suggested by this study showed the maximum error percentage of less than 4.3% compared with $REWS_{power}$ under high wind speed conditions, the method could derive significantly more accurate results than nacelle wind speeds under all of the other conditions. Therefore, it can be applied instead of the point wind speed when predicting the AEP of wind turbines affected by wakes. More importantly, this method could be

Table 2
Rotor segmented areas and weighting values to determine $REWS_{spws}$.

Segment symbol	Segment area [m^2]	Weighting value [%]
A_1	1885	37.5
A_2	628	12.5
A_3	628	12.5
A_4	1885	37.5
Total area	5026	-

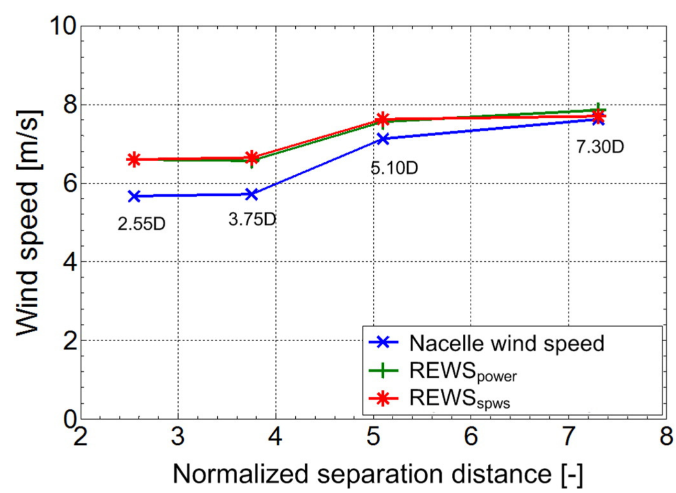

Fig. 14. Comparison between the nacelle wind speed, $REWS_{power}$, and $REWS_{spws}$ ($V_{freestream}$: 8.5 m/s–9.5 m/s).

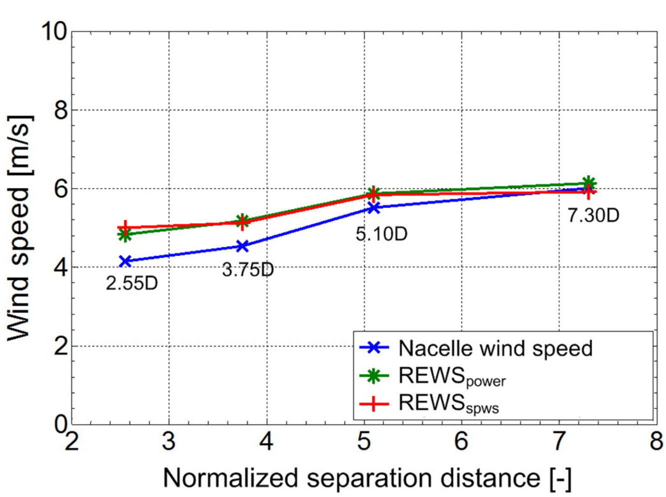

Fig. 13. Comparison between the nacelle wind speed, $REWS_{power}$, and $REWS_{spws}$ ($V_{freestream}$: 6.5 m/s–7.5 m/s).

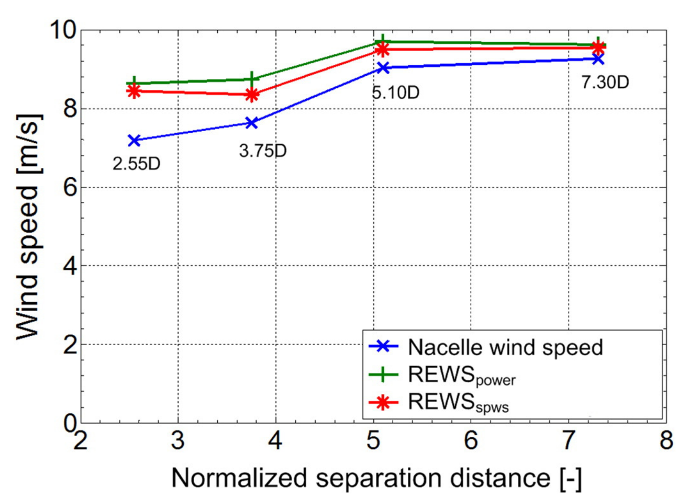

Fig. 15. Comparison between the nacelle wind speed, $REWS_{power}$, and $REWS_{spws}$ ($V_{freestream}$: 10.5 m/s–11.5 m/s).

more accurate in predicting wake loss occurring under low wind speed and near wake conditions and incorporate this loss in AEP calculations.

Conclusions

In order to increase the prediction accuracy of wake loss in downstream wind turbines affected by wakes, this study proposes a method to calculate the rotor equivalent wind speed in consideration of wake wind shear. Differences between the point wind speed, $REWS_{power}$, and $REWS_{spws}$ were compared and analyzed to examine the method's applicability. The nacelle wind speed was used as the point wind speed, and by comparing $REWS_{power}$ and $REWS_{spws}$ calculated from the power output and the nacelle wind speed measured from the actual wind farm, respectively, the following conclusions were obtained:

1) The difference between the point wind speed and $REWS_{power}$ measured at the hub height was widest in the wake center region and showed maximum error percentages of 9% and 3% in the near and far wake regions, respectively. Furthermore, as the speed of wind flowing into upstream wind turbines decreased, the difference between the two wind speeds increased. Conversely, as the incoming wind speed increased, the difference decreased.
2) By applying the REWS discussed in IEC61400-12-1, this study suggested a $REWS_{spws}$ calculation method applicable to wind turbines affected by wakes, and examined its applicability through comparison between $REWS_{power}$ and $REWS_{spws}$ calculation results. Under near wake and low wind speed conditions, the $REWS_{spws}$ calculation method was verified as sufficiently accurate. Although it overestimated compared to $REWS_{power}$ under far wake and high wind speed conditions, its prediction accuracy was notably higher than that of the point wind speed.
3) When calculating the wake loss and AEP of wind turbines affected by wakes, the $REWS_{spws}$ model suggested in this study should be applied to increase the accuracy of calculation results, rather than applying the point wind speed derived from a certain wake profile point by using wake models.

Acknowledgment

This study was supported by “Development of multi-class large capacity wind power generator system specialized in Korea wind site” of the Korea Institute of Energy Technology Evaluation and Planning (KETEP), granted financial resource from the Ministry of Trade, Industry & Energy, Republic of Korea (No. 20173010024930).

References

Ainslie JF. Calculating the flow field in the wake of wind turbines. J Wind Eng Ind Aerodyn 1988;27:213–24.

Barth V, Wassie Tsegai A. Micrositing using rotor equivalent wind speed. DEWI Mag 2014, August(45). Available at: http://www.dewi.de/dewi_res/fileadmin/pdf/publications/Magazin_45/02.pdf.

Barthelmie RJ, Pryor SC, Frandsen ST, Hansen KS, Schepers JG, Rados K, et al. Quantifying the impact of wind turbine wakes on power output at offshore wind farms. J Atmos Oceanic Tech 2010;27:1302–17.

Clifton A, Kilcher L, Lundquist J, Fleming P. Using machine learning to predict wind turbine power output. Environ Res Lett 2013;8, 024009.

EMD International A/S. Available at: http://help.emd.dk/knowledgebase/default.aspx.

Gaumond M, Rethore P-E, Bechmann A, Ott S, Larsen GC, Pena A, et al. Benchmarking of wind turbine wake models in large offshore wind farms. Proceedings of the science of making torque from wind conference, Oldenburg; 2012. Available at: http://www.eera-dtoc.eu/wp-content/uploads/files/Gaumond-et-al-Benchmarking-of-wind-turbine-wake-models-in-large-offshore-wind-farms5.pdf.

IEC 61400-12-1. Wind turbines – part 12–1: power performance measurements of electricity producing wind turbines. International Electrotechnical Commission; 2013.

Jensen NO. A note on wind generator interaction. Tech. Report. Riso-M-2411(EN). Riso National Laboratory; 1983. Available at: http://orbit.dtu.dk/files/55857682/ris_m_2411.pdf.

Jeon Sanghyeon, Kim Bumsuk, Huh Jongchul. Comparison and verification of wake models in an onshore wind farm considering single wake condition of the 2MW wind turbine. Energy 2015;93:1769–77.

Katic I, Højstrup J, Jensen NO. A simple model for cluster efficient. EWEA conference; 1986. p. 407–10.

Larsen GC. A simple wake calculation procedure. Tech. Report. Riso-M-2760(EN). Riso National Laboratory; 1988. Available at: http://orbit.dtu.dk/files/55567186/ris_m_2760.pdf.

Machielse LAH, Eecen PJ, Korterink H, van ser Pijl SP, Schepers JG. ECN test farm measurements for validation of wake models. Tech. Report. ECN-M–07-044. Energy research Center of the Netherlands; 2007. Available at: ftp://ftp.ecn.nl/pub/www/library/report/2007/m07044.pdf.

Mckay Phillip, Carriveau Rupp, Ting David S-K, Newson Timothy. Turbine wake dynamics. InTech; 2012. Available at: http://cdn.intechopen.com/pdfs-wm/40860.pdf.

Moriarty Patrick, Rodrigo Javier Sanz, Gancarski Pawel, Chuchfield Matthew, Naughton Jonathan W, Hansen Kurt S, et al. IEA-task 31 WAKEBENCH: towards a protocol for wind farm flow model evaluation. Part 2: wind farm wake models. J Phys 2014. Conference Series, volume 524, conference 1. Available at: http://iopscience.iop.org/article/10.1088/1742-6596/524/1/012185/pdf.

Sanderse B. Aerodynamics of wind turbine wakes. Tech. Report. ECN-E-09-016. Energy research Centre of Netherlands; 2009. Available at: http://www.ecn.nl/docs/library/report/2009/e09016.pdf.

Schepers JG, Obdam TS, Prospathopoulos J. Analysis of wake measurements from the ECN wind turbine test site Wieringermeer. EWTW Wind Energy 2012;15(4):575–91.

Sørensen Thomas, Thøgersen Morten Lybech, Nielsen Per. Adapting and calibration of existing wake models to meet the conditions offshore wind farms. Aalborg: EMD International A/S; 2008. Available at http://energinet.dk/SiteCollectionDocuments/Danske%20dokumenter/Forskning%20-%20PSO-projekter/5899%20Tilpasning%20og%20kalibrering%20af%20eksisterende%20skyggevirkningsmodeller.pdf.

VanLuvanee David Ryan. Investigation of observed and modeled wake effects at horns rev using WindPRO. Master thesis at the technical University of Denmark, 25 August; 2006. Available at: http://www.mek.dtu.dk/~/media/Institutter/Mekanik/Sektioner/FVM/uddannelse/eksamensprojekt/mastertheses%20fm/david_ryan_vanlucanee_mek_fm_ep_2006_05.ashx.

Wagner R, Antoniou I, Pedersen SM, Courtney MS, Jørgensen HE. The influence of the wind speed profile on wind turbine performance measurements. Wind Energy 2009;12:348–62.

Wagner R, Courtney M, Gottschall J, Lindelöw-Marsden P. Accounting for the speed shear in wind turbine power performance measurement. Wind Energy 2011; 14:993–1004.